



THE NONLINEAR DYNAMICS OF THE CRAYFISH MECHANORECEPTOR SYSTEM

SONYA BAHAR* and FRANK MOSS†

*Center for Neurodynamics, University of Missouri at St. Louis,
 St. Louis, MO 63121, USA*

**ssb2001@med.cornell.edu*

†*mossf@umsl.edu*

Received June 6, 2002

We review here the nonlinear dynamical properties of the crayfish mechanoreceptor system from the hydrodynamically sensitive hairs on the tailfan through the caudal photoreceptor neurons embedded in the 6th ganglion. Emphasis is on the extraction of low dimensional behavior from the random processes (noise) that dominate this neural system. We begin with stochastic resonance in the sensory root afferents and continue with a discussion of the photoreceptor oscillator and its instabilities. Stochastic synchronization, rectification and the generation of second harmonic responses in the photoreceptors are finally discussed.

Keywords: Stochastic synchronization; stochastic resonance; neuronal dynamics; crayfish mechanoreceptor.

1. Introduction

The crayfish is a venerable animal, and a successful one, having spread over the globe from the arctic to the tropics. There are at least 590 species of crayfish and they are found presently on all continents except Africa and Antarctica [Ortmann, 1902; Crandall & Fetzner, 2002]. However, fossils from Antarctica demonstrate that crayfish also lived there almost 300 million years ago. In North America (Wyoming, Utah, Arizona and North Carolina) crayfish were present at least 225 million years ago on the Pangean continent [Packard, 1880; Olsen, 1977; Miller & Ash, 1988; Hasiotis, 1999].

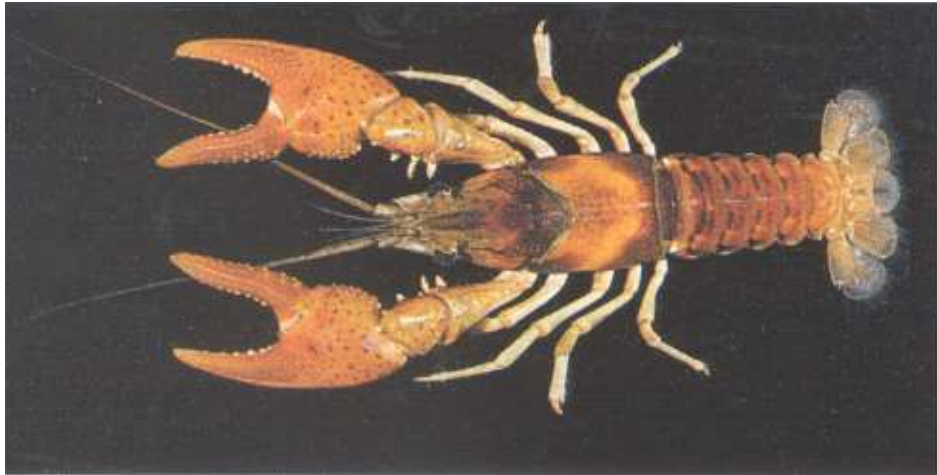
Aristotle first identified crayfish (*astakoi*) and distinguished them from lobsters, shrimps and crabs [Aristotle, 322 BC]. But it was Thomas Henry Huxley who made the animal familiar to biologists by introducing the modern study of physiology (then called zoology) using the crayfish as an example

[Huxley, 1880]. The first neuroscience studies on crayfish involving the measurement of neural action potentials were carried out in the thirties [Prosser, 1934; Welsh, 1934].

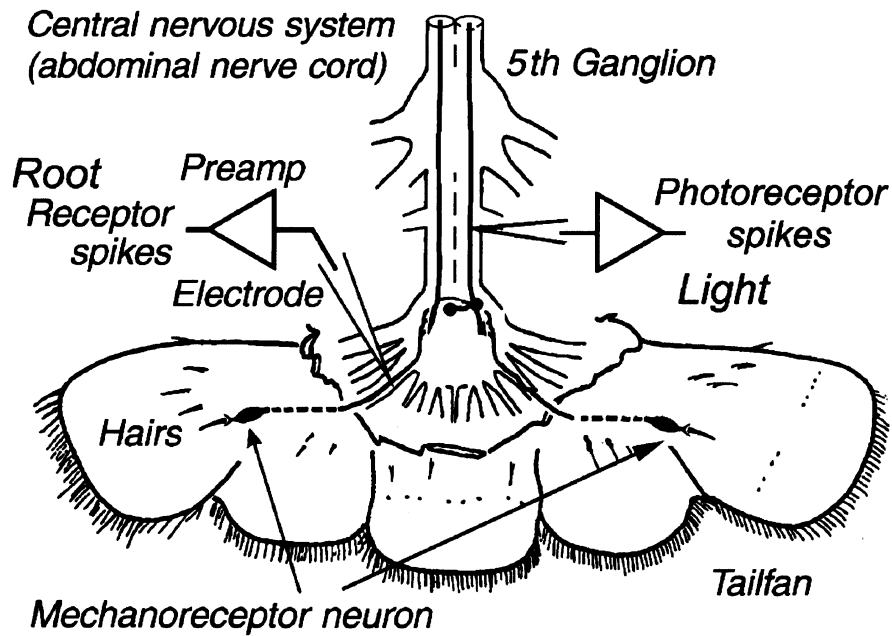
Here we focus on the lower parts of the crayfish mechanosensory system, specifically the tailfan and the sixth abdominal ganglion. The tailfan is covered with thousands of hydrodynamically sensitive hairs. They are divided into two broad groups, some 250 long hairs (about 100 by 10 μm) that sense water motions in the frequency range 4 to 20 Hz and myriad short ones (about 10 μm) that sense acoustic vibrations in a higher frequency range [Plummer *et al.*, 1986; Douglass & Wilkens, 1998].

Here we are concerned with the long hairs, each of which is innervated by two sensory afferent neurons that converge on the sixth ganglion and synapse on some of the approximately 250 interneurons that comprise the ganglion [Flood & Wilkens, 1978; Wiese, 1976]. We are also interested in the two

*Current address: Department of Neurological Surgery, Weill-Cornell Medical College, 525 East 68th St., Box 99, New York, NY 10021, USA.



(a)



(b)

Fig. 1. (a) The Mammoth Spring Crayfish *Orconectes marchandi* (Hobbs). Reprinted from *Missouri Conservationist* with permission of the Missouri Department of Conservation. Original photograph by William L. Pflieger. (b) Diagram of the tailfan, sixth ganglion and the caudal photoreceptors showing the neural connectivity and recording sites.

bilaterally symmetric photoreceptor neurons, called the caudal photoreceptors (CPRs), embedded in the ganglion and synaptically connected to some of its interneurons [Welsh, 1934; Kennedy, 1958a, 1958b, 1963; Wilkens & Larimer, 1972]. See Fig. 1.

In addition to the two CPR neurons and many others, the ganglion outputs a pair of motor neurons that cause the abdominal muscles to contract.

To escape a predator, the crayfish spreads its tailfan and contracts its abdominal muscles resulting in a swift backward swimming motion called the escape reflex [Krasne & Wine, 1975; Wine, 1977, 1984]. Together, these two organs, the tailfan and the sixth ganglion, form a system for exciting the escape reflex of the crayfish. Hydrodynamic motions applied to the long hairs, and light falling

on the CPRs, mediate the neural outputs of the ganglion. Hydrodynamic motions trigger the escape reflex, and light intensity can, as we will show below, enhance the transduction of mechanosensory stimuli. Furthermore, it is known that light directly mediates some reflex behaviors in the crayfish, such as backwards walking [Edwards, 1984; Simon & Edwards, 1990]. (Interestingly, some investigators report that backward walking can *inhibit* the escape response [Phillips & Edwards, 1986].) The escape reflex is designed for escape from predators, chiefly swimming fish. The wave-like disturbances in the water due to the fish's swimming motions arrive at the tailfan in advance of the fish triggering the escape reflex with some probability, depending in part on the stochastic firing of the neurons that innervate the mechanosensory hairs. Once triggered, the crayfish may escape the predator also with some probability. As we argue below, the entire escape process is statistical.

This predator avoidance system seems primitive, though it is enormously sensitive [Douglass *et al.*, 1993]. The widespread diffusion of the many species indicates that it is evidently a very successful system as well. One can speculate that hairs moving in response to water motions may have been one of the earliest responses to the appearance of predators in the pre-Cambrian seas.

In this overview, we outline the results of a number of experiments aimed at revealing some of the nonlinear processes involved in the transduction of hydrodynamic signals into nerve impulse trains in the CPR outputs. The experiments were all performed following the same protocols. Periodic and sometimes random hydrodynamic stimuli were applied to the tailfan, while the light sensitive areas of the CPRs on the ganglion surface were illuminated or remained in the dark. Recordings of the neural discharges were made by means of electrodes attached extracellularly either to the sensory afferents or to the CPR outputs as shown in Fig. 1(b). Owing to the extreme vibration sensitivity of the tailfan, all experiments were performed on vibration isolation platforms within grounded Faraday cages under conditions of controlled illumination and temperature. Trains of neural action potentials, or spike trains, were digitized, saved and later analyzed, as will be discussed below (Sec. 5.3).

In Sec. 2 we discuss first the nature of the stimuli, oscillatory responses and noise. Then we further discuss the role of light and its relation to noise. Section 3 outlines the first Stochastic

Resonance (SR) experiment in biology and points to the many further works that it stimulated. In this section we also outline the threshold theory of SR and elucidate why it has been so successful and where it fails. Section 4 deals with stable and unstable orbits of a noisy oscillator (the illuminated CPR). In Sec. 5, we introduce the very modern topic of Stochastic Synchronization (SS) and outline how it can be used to investigate the encoding in the CPRs of periodic hydrodynamic stimuli applied to the tailfan. Section 6 deals with the rectification and summation of oscillatory mechanostimuli by the CPRs. Here we introduce a simple model — albeit linear — for this process. A related topic treated here is the generation under certain conditions of a strong second harmonic in the CPR responses and its mediation by light. We conclude with a speculation on the possible functional significance of rectification and the consequent generation of higher harmonics. Finally in Sec. 7, we conclude with a discussion pointing to possible future directions for research on this intriguing sensory system.

Two useful sites on the World Wide Web covering all aspects of crayfish research, conservation and natural history are the Smithsonian Museum of Natural History [2001] and [Crandall & Fetzer, 2002].

2. Signals, Oscillations and Noise

We consider first the spontaneous discharges from the sensory afferents, often called the sensory root receptors. Recordings were made from the electrode and amplifier shown on the left in Fig. 1(b). The root sensory afferents are far from silent even in the absence of external stimuli. Figure 2(a) shows an interspike interval histogram measured on a sensory afferent root. The dashed line shows an exponential fit to the data. The fit indicates that the intervals are gamma-function distributed. The exponential part is evidence of a Poisson process, that is, the signature of random noise.

While the spontaneous discharges from all sensory afferent neurons show firings at random times, some are much more noisy than others as indicated by relatively high mean firing rates. Others are nearly silent. Several hundred afferents (from the long hairs alone) and their noisy discharges converge on the sixth ganglion and synapse onto the CPRs. Thus it is not surprising that the CPRs are also quite noisy.

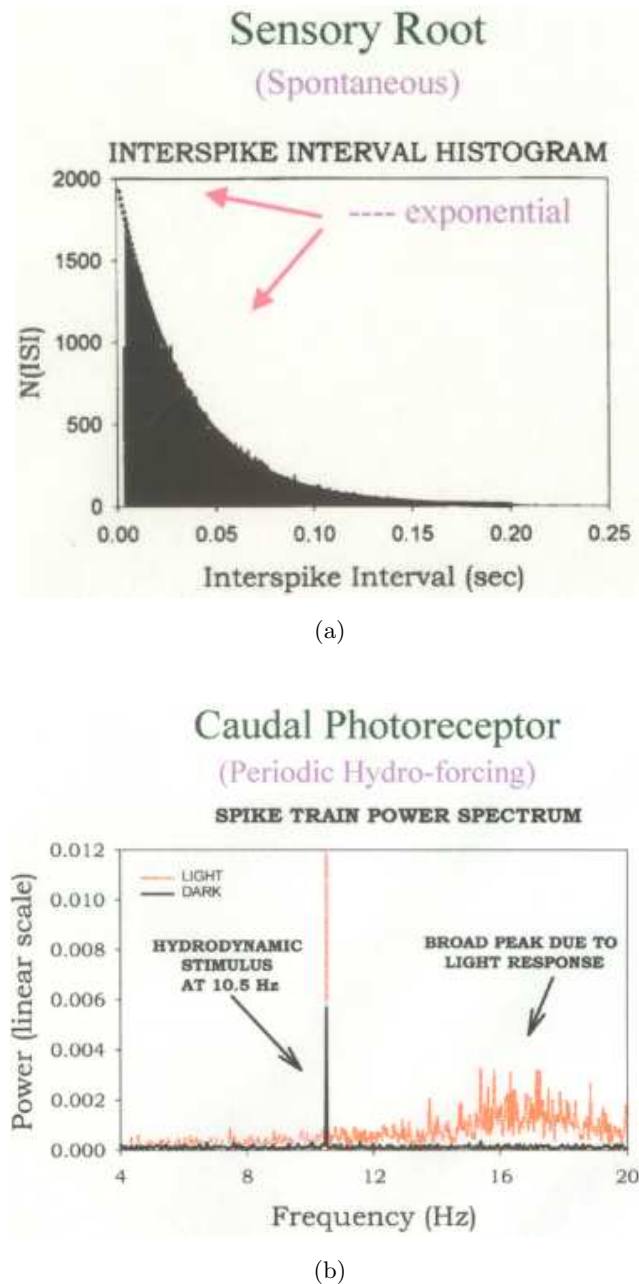


Fig. 2. (a) Interspike interval histogram of spontaneous discharge from a selected crayfish neuron in the sensory root in the absence of stimulation. Dashed line in color is a fit to an exponential. The short time cut-off results from the approximately 2.5 ms refractory time for sensory afferents. (b) Power spectra of discharges measured at the CPR output in dark (black) and light (color) with 10.5 Hz periodic hydrodynamic stimulation applied to the tailfan.

But the CPR neurons are also oscillators [Bruno & Kennedy, 1962; Kennedy 1958a, 1958b, 1963], though very noisy ones. Moreover the oscillatory behavior is mediated by the steady

light intensity falling on the CPR sensitive areas. Figure 2(b) shows two power spectra measured at a CPR output. See the right-hand electrode and amplifier in Fig. 1(b). The broad peak in the light lying between approximately 14 to 20 Hz is the CPR oscillator, and we may speculate that the broadness of the peak is due to in part to spontaneous noise converging on the ganglion from the root afferents. Synchronization of the CPR oscillators with external hydrodynamic forcing is discussed in Sec. 5. The sharp peaks at 10.5 Hz are the result of periodic hydrodynamic stimulation. We note that light considerably enhances the amplitude of the 10.5 Hz peak, an effect that is further discussed in Sec. 3.2.

3. Stochastic Resonance

Stochastic resonance (SR) is the now well-studied process by which the addition of noise to a weak signal in a class of nonlinear systems can enhance the detectability and information content of the processed signal downstream. Though first studied in dynamical physical systems and demonstrated experimentally in a bistable ring laser [McNamara *et al.*, 1988], SR has had its major impact in biology and more recently in medicine. With its first biological demonstration, SR was discovered in the mechanosensory system of the crayfish [Douglass *et al.*, 1993]. SR has been the subject of numerous reviews [Moss, 1994; Moss *et al.*, 1994; Wiesenfeld & Moss, 1995; Gammaitoni *et al.*, 1998, Anishchenko *et al.*, 1999; Moss, 2000]. Here, we will only briefly outline the process.

In its original manifestation SR was thought to occur only in dynamical systems incorporating a bistable potential [Gammaitoni *et al.*, 1998]. Subject to a weak signal that “rocked” the bistable potential periodically and noise, the system state point (often described as a “particle”) passed over the barrier from one well to the other. These barrier crossings are to some degree random, but also to some degree synchronized with the periodic rocking signal. Quite early it was realized that the barrier crossings themselves represented a significant source of information about the signal, and that the information could have biological significance [Longtin *et al.*, 1991].

In an alternate view, it was later discovered that SR can exist in *nondynamical*, purely statistical, systems consisting of only three ingredients:

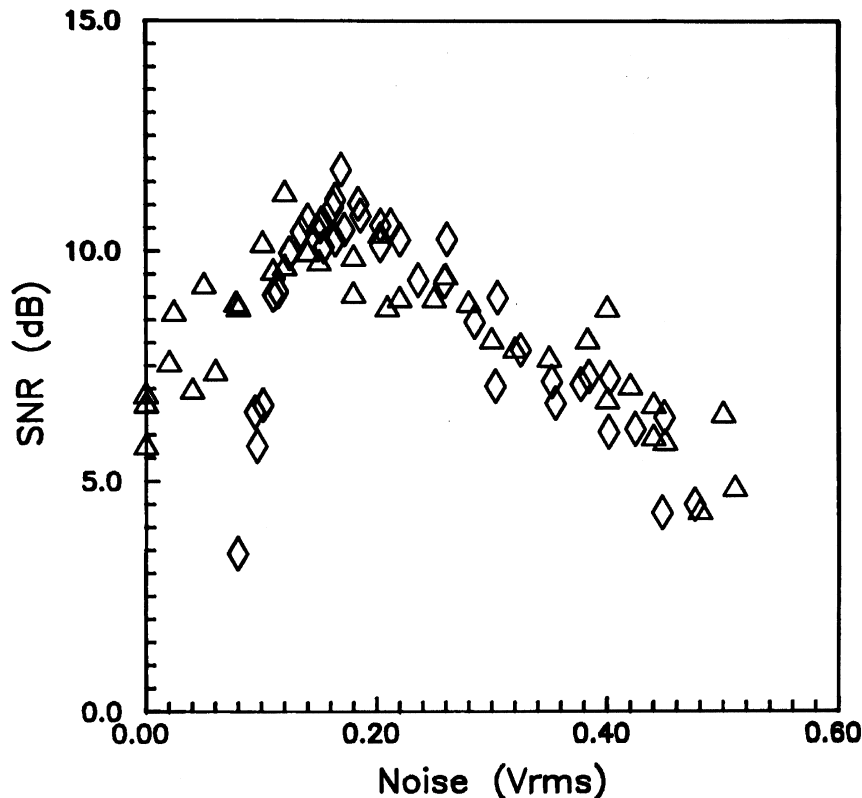


Fig. 3. The signal-to-noise ratio (SNR) versus noise measured at a root sensory afferent of the crayfish (triangles) while stimulating with a hydrodynamic stimulus composed of a subthreshold periodic signal plus random noise. The horizontal scale is in root mean square voltage applied to an electromechanical motion transducer and is proportional to amplitude of motion of the tailfan relative to a liquid solution in which it was immersed. The diamonds show a similar experiment carried out on an analog simulator of a model FitzHugh–Nagumo neuron with parameters chosen to yield data similar to that of the crayfish.

a threshold, a subthreshold signal and noise [Gingl *et al.*, 1995; Moss *et al.*, 1994]. The signal detection paradigm is equally simple. We suppose that the system can output a temporal sequence of positive going threshold crossings. When the threshold is not crossed there is no output. When the subthreshold signal plus the noise causes a barrier crossing, the system outputs a stereotypical pulse (a marker). The train of such pulses is similar to the discharges of many neurons and carries a surprising amount of information about the subthreshold signal. The information is maximized at optimal noise intensity. Too little noise and the signal is not sampled adequately; too much and the signal is swamped with noise. In both cases, the information content is degraded. A classical measure of the information content in such a pulse train is the signal-to-noise ratio (SNR), though other measures have been adopted, suitable for behavioral data [Freund *et al.*, 2002; Greenwood *et al.*, 2000; Russell *et al.*, 1999;

Ward *et al.*, 2002] or for theories on cell membrane ion channels [Goychuk & Hänggi, 2000].

The signature of SR is that the information measure, for example the SNR, attains its maximum value at the optimal noise intensity. An example from the original experiment with the crayfish mechanosensory system [Douglass *et al.*, 1993] is shown in Fig. 3. The triangles are SNRs measured from an afferent root compared with diamonds from a simulation of a noisy FitzHugh–Nagumo model neuron [Moss *et al.*, 1993].

3.1. *SR mediated by light in the CPRs*

We now consider SR experiments carried out in the CPR neurons and the effects of light on transduction of the hydrodynamic signal. Figure 2(b) shows that a 10.5 Hz hydrodynamic signal is transduced in the CPRs with greater efficiency in the light as compared to that measured in the dark. The SNR

of the 10.5 Hz signals appearing in these two power spectra is simply the ratio of the area under the peak to the area in a 1 Hz bandwidth of the noise background centered on the frequency of the stimulus. We can see that the SNR is much greater in the presence of light.

A systematic study of light enhancement of hydrodynamic signals in the CPR neurons has been carried out [Pei *et al.*, 1996]. Signatures similar to SR were observed, that is the SNR was found to pass through a maximum at an optimal light intensity. This observation raises the question, as yet unresolved, as to whether the light generates noise in the CPR and acts in concert with an inherent threshold to result in the SR signature. Another question, also unresolved, is how the animal might make use of the light-enhancement effect. We have advanced a speculation [Pei *et al.*, 1996] based on the notion that the spontaneous neural firing of the mechanosensory neurons and the CPRs are primarily statistical by nature, and that evolution has acted to optimize the statistics and ultimately the animal's survival probabilities. The crayfish is primarily a nocturnal creature spending most days within a burrow. It does sometimes, however, emerge from the burrow in the daylight to forage. During such times it is available to predators, and the mechanosensory "early warning system" should be at maximum sensitivity. Hence the light enhanced SNRs. By contrast, when safely within its burrow (in the dark) it is necessary to "shut down" the system in order to reduce the probability of accidental triggers of the escape reflex, some of which might cause the animal to exit the burrow thus becoming susceptible to predators.

Light has an effect also on the quality of synchronization between the external hydrodynamic stimulus and the CPR discharges. Studies on light mediated SS and its relation to SR are detailed in Sec. 5.

4. Stabilities and Instabilities

Dissipative chaos is built upon a structure of a countable infinity of Unstable Periodic Orbits (UPOs) [Artuso *et al.*, 1990a, 1990b]. An illustration of such an orbit (of period-1) is depicted in Fig. 4(a). Recurring orbits (solid and dashed curves) encounter a saddle-shaped potential characterized by stable and unstable manifolds that intersect at the unstable periodic point (UPP) (at the bottom of the straight dashed line at the center of the sad-

dle). Upon each recurrence, the orbit intersects the top section as marked by the colored circles. If the orbit lands near the stable manifold it will be drawn toward the UPP on its successive recurrences following the stable manifold (red circles). But the UPP is unstable and near it, the orbit senses the presence of the unstable manifold. It thence departs along the unstable direction (green points).

Neurons that fire recurrently can show UPOs that are experimentally detectable by certain sequences of interspike time intervals marking the approaches and departures along the stable and unstable directions. An example is depicted in Fig. 4(b). The experimental detection of UPOs has been discussed and demonstrated in physical and biological systems [Pierson & Moss, 1995]. The orbits were first detected in sensory biology in the oscillators of the crayfish CPRs with periodic hydrodynamic forcing [Pei & Moss, 1996]. In noisy systems, such as the crayfish CPRs, only orbits of low period are detectable owing to the exponential scaling of their occurrence probability with period [Pei *et al.*, 1998].

Precursors of period-doubling bifurcation have also been detected with algorithms similar to those for detecting UPOs [Omberg *et al.*, 2000]. UPOs in dynamical systems also occur during a period-doubling process whereby successive stable periodic orbits lose stability at the bifurcations becoming UPOs beyond. UPOs and the precursors of period-doubling bifurcations have been extensively observed by the group of H. A. Braun in several neural systems including temperature dependent catfish electroreceptors [Braun *et al.*, 1997] and rat cold receptors [Braun *et al.*, 1999a] and hypothalamic neurons in rat brain slice preparations [Braun *et al.*, 1999b].

In the crayfish CPR neurons with periodic hydrodynamic forcing, the UPOs show up for certain conditions of forcing amplitude and frequency when the CPR is illuminated. A mapping of the UPO density in the CPRs over ranges of these variables has been provided for the period-1 orbits [Pei & Moss, 1996]. Higher order orbits have also been detected in the crayfish CPR [Pei *et al.*, 1998]. What the appearance of UPOs may mean to the animal, if anything, is unknown at this time.

5. Stochastic Synchronization

Synchronization is the process whereby a nonlinear oscillator may slightly shift its natural frequency to

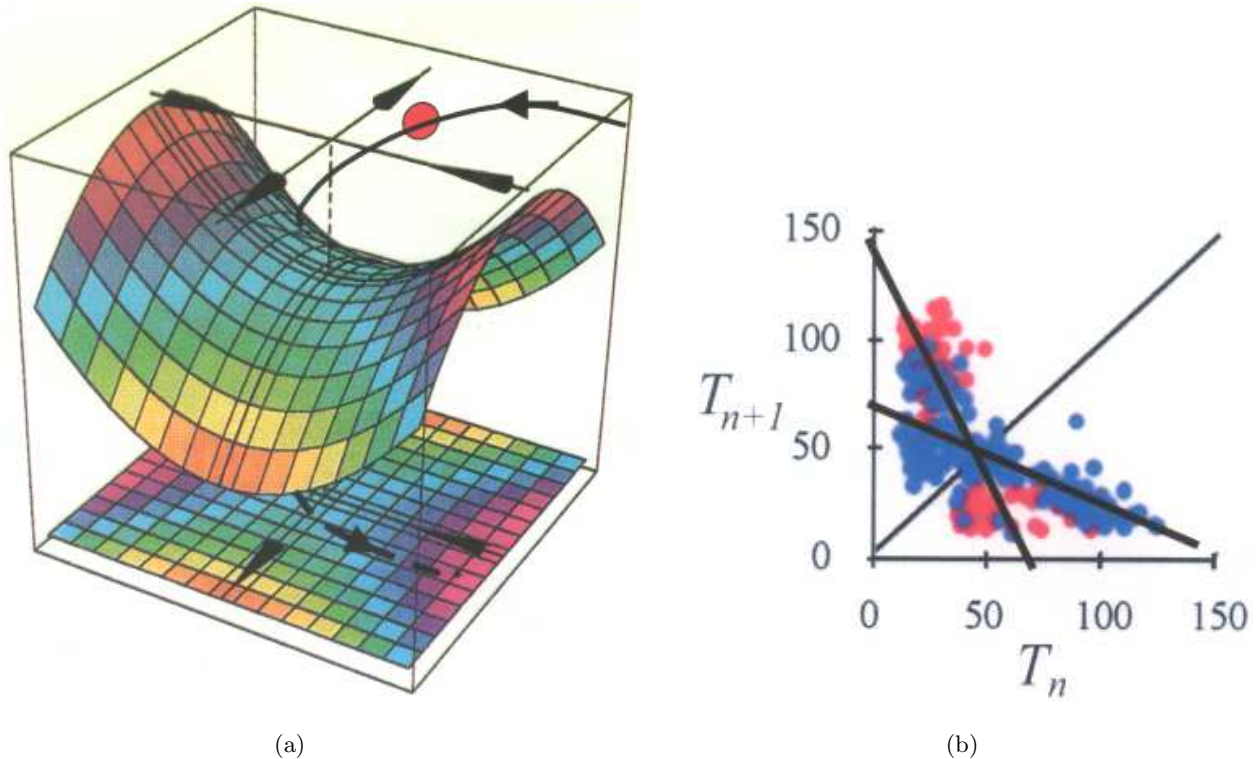


Fig. 4. (a) A saddle potential. The unstable periodic point (UPP) is at the center (end of vertical dashed line). Stable and unstable manifolds are indicated by the inward and outward pointing arrows on the top face. Penetrations of the top face by the unstable periodic orbits (UPOs) are marked by the circles (red follow the stable manifold toward the UPP, green depart along the unstable manifold) in numbered sequence. Adapted from [Moss, 1994b]. (b) A Poincaré section, first return map, showing successive time intervals between the returns of the orbits. Stable and unstable manifolds are indicated by the straight lines with inward and outward pointing arrows respectively. They intersect at the UPP. Time intervals between successive neural action potentials are marked by the colored dots. UPOs of period- q are detected in return maps, T_{n+q} versus T_n .

coincide with that of a driving oscillator. The difference in phases of the two oscillators then becomes constant in time. Stochastic Synchronization (SS) refers to this process when there is noise present in one or both oscillators. They can then synchronize for a time, then drop out of the phase locked condition. The episodes of phase locking and slip-page occur randomly. The field of SS is devoted to characterizing this random process in various nonlinear systems including biological ones.

5.1. Synchronization of a noisy oscillator with a hydrodynamic signal

Scientific interest in the synchronization of oscillating physical systems, such as clock pendula, dates back to the work of Huygens [1673]. More recently, it has been realized that many biological systems — circadian rhythms, heart rate, neural firing, calcium oscillations, etc. — are oscillatory

as well. But a problem arises when one seeks to study synchronization in oscillating biological systems: these systems are notoriously noisy. The study of synchronization of biological systems was facilitated by the pioneering work of Stratonovich [1967] on the synchronization of stochastic oscillating systems. This was later extended with studies of synchronization between the *phases* of noisy oscillators [Rosenblum *et al.*, 1996; Neiman *et al.*, 1999a; Pikovsky *et al.*, 2001; Rosenblum *et al.*, 2001], studies of synchronization-like phenomena in coupled bistable systems [Neiman, 1994], and other work (see [Pikovsky *et al.*, 2001] for review). Particularly relevant in our case is the fact that, in stochastic phase synchronization of biological oscillators, actual phase entrainment will typically persist for only a few cycles at a time. This necessitates the assessment of synchronization using *statistical measures* [Neiman *et al.*, 1999b, 2000].

With a theory of stochastic phase synchronization firmly in place, experimental observations

of biological synchronization have accumulated quickly in recent years. For example, Schäfer *et al.* [1998a, 1998b] characterized the synchronization between breathing and heartbeat. Tass *et al.* [1998] demonstrated increased synchronization between cortical firing and muscle activity in Parkinsonian patients. Neiman *et al.* [1999b, 2000] observed synchronization in the electrosensitive afferent neurons of the paddlefish.

A further motivation for using synchronization methods is that these techniques provide much more information than more traditional cross-spectral methods. Phase synchronization methods are not equivalent to cross-spectral techniques; in fact they provide a much stronger measure than the cross correlation. As pointed out by Tass *et al.* [1998] and Rosenblum *et al.* [2001], if two systems synchronize, their signals are correlated; the reverse case does not hold. Synchronization allows one to follow two systems, or a system and a stimulus, as they remain entrained over a range of frequencies. Cross correlation and related measures do not contain information about the time-evolution of the phase difference between two signals, while this information is front and center in phase synchronization analysis. Synchronization measures, such as the synchronization index defined below, allow the identification of various frequency-locking regimes, information which is not contained in cross-spectral methods. By measuring synchronization, therefore, it is possible to obtain detailed information about the time-variation of the entrainment between a stimulus and response, as well as the type of mode-locking between the two signals, and the behavior of their entrainment as the driving frequency is varied.

As discussed above, the crayfish caudal photoreceptors (CPRs) are both *primary* light sensors and *secondary* interneurons in a mechanosensory (hydrodynamic) pathway. The crayfish can detect water motions as small as 20 nm [Plummer *et al.*, 1984], and is thought to use this exquisite sensitivity for predator avoidance [Pei *et al.*, 1996]. Mechanosensory hairs on the crayfish tailfan are mechanically coupled to sensory neurons whose axons enter the sixth abdominal ganglion [Wilkins & Larimer, 1972; Wiese, 1976; Wiese *et al.*, 1976; Wilkins, 1988], as shown in Fig. 1(b). These neurons synapse onto the CPR cells. Thus, recording extracellularly from the axons of one or both of the CPRs, the response to light

or to periodic mechanical stimuli may be observed, depending on the experimental conditions [Flood & Wilkins, 1978; Douglass & Wilkins, 1998].

One of our interests has been the determination of the *mechanism* by which the mechanosensory stimulus is encoded. In particular, as we review here, we have shown that *stochastic phase synchronization* occurs between the photoreceptor firing and a periodic (sinusoidal) hydrodynamic stimulus. It is known that the direction in which the mechanosensory hairs are bent (and thus the phase of a mechanical stimulus) triggers the firing of the afferent neurons to which they are mechanically coupled [Wiese, 1976; Wiese *et al.*, 1976]. Thus some phase relationship between the stimulus and response is to be expected. Indeed, recordings from the photoreceptor [Flood & Wilkins, 1978] and the mechanoreceptor (sensory root) neurons [Wiese, 1976; Wiese *et al.*, 1976] show well-defined clumps of neural spikes in what appears to be a fixed phase relationship with the stimulus.

But this is not sufficient to demonstrate synchronization. As Rosenblum *et al.* [2001] pointed out, synchronization is a process, not a state. This means that in order to demonstrate that the mechanosensory system encodes hydrodynamic signals by directly synchronizing with the stimulus frequency, it is necessary to demonstrate frequency locking between the stimulus and response *over a range of frequencies*. As discussed in Sec. 5.4, this does indeed occur in the CPR system. But before discussing the experimental results, however, we must pause to review some of the theoretical basis of stochastic phase synchronization, as well as the experimental methods used in our experiments.

5.2. *Theory: The synchronization index*

If the CPR's firing times are denoted as t_k , $k = 0, 1, 2, \dots, N$, and the upward zero-crossing times of the applied periodic stimulus as τ_i , $i = 0, 1, 2, \dots, M$, then the phase difference of the k th spike with respect to the stimulus is

$$\phi(t_k) = 2\pi \frac{(t_k - \tau_i)}{\tau_{i+1} - \tau_i} \quad (1)$$

where $\tau_i < t_k < \tau_{i+1}$ [Neiman *et al.*, 1999b; Rosenblum *et al.*, 2001; Neiman *et al.*, 2000; Pikovsky *et al.*, 2001]. $\phi(t_k)$ will have values between 0 and 2π . (A similar phase difference measure may be calculated between two different spiking neurons,

where τ_i , instead of the zero-crossing times of the stimulus, represents the firing times of the second neuron.) The *continuous* phase difference, which can fall between 0 and infinity, rather than being “wrapped” modulo 2π , can be defined at time t as

$$\phi(t) = 2\pi \frac{(t - \tau_1)}{\tau_{i+1} - \tau_i} + 2\pi i \quad (2)$$

where $\tau_i < t < \tau_{i+1}$ and i is the stimulus cycle number, and, as before, the τ_i , $i = 0, 1, 2, \dots, N$ are the upward x -axis crossings of the applied stimulus [Neiman *et al.*, 1999b; Neiman *et al.*, 2000; Rosenblum *et al.*, 2001; Pikovsky *et al.*, 2001].

If a neuron fires m times during n stimulus cycles, the $n:m$ phase locking condition is

$$|n\phi(t) - m\phi_{\text{stim}}(t) - \delta| < \text{const.} \quad (3)$$

for the ideal case where there is no noise in the system. Here, $\phi(t)$ is the phase of the neural firing given in Eq. (2), $\phi_{\text{stim}}(t) = 2\pi f_0 t$ is the continuous phase of the stimulus, and δ is the average phase shift between the two signals [Rosenblum *et al.*, 2001]. When condition (3) holds, the oscillator (neuron) and driving stimulus are said to be $n:m$ phase locked, and the $n:m$ phase difference is defined as

$$\Phi_{n,m}(t) = \left[2\pi \frac{(t - \tau_i)}{(\tau_{i+1} - \tau_i)} + 2\pi i \right] n - 2\pi m f_0 t \quad (4)$$

The corresponding frequency entrainment condition is

$$nf = mf_0, \quad (4a)$$

recalling that the frequency f and phase ϕ of a periodic oscillator are related as

$$f = \frac{1}{2\pi} \frac{d\phi}{dt}. \quad (4b)$$

In this case one can make the statement that phase synchronization and frequency entrainment are two different ways of describing the same condition.

In a noisy system, the phase difference (3) becomes unbounded, and we can speak of synchronization only in a statistical sense. In this case frequency entrainment occurs only during the brief intervals where $\phi(t)$ remains constant between phase slips (where, due to noise, $\phi(t)$ abruptly changes by $\pm 2\pi$). Even though frequency entrainment may only hold for brief periods of time in a noisy system, the quality of synchronization in a statistical sense may be found by plotting the probability density of the phase differences (4).

The intensity of the first Fourier mode of this distribution,

$$\gamma_{n,m}^2 = \langle \cos(\Phi_{n,m}(t)) \rangle^2 + \langle \sin(\Phi_{n,m}(t)) \rangle^2, \quad (5)$$

where $\langle \cos(\Phi_{n,m}(t)) \rangle^2$ and $\langle \sin(\Phi_{n,m}(t)) \rangle^2$ are time averages, defines the synchronization index $\gamma_{n,m}$, which varies from 0 to 1 and is indicative of the relative strength of $n:m$ mode locking [Rosenblum *et al.*, 2001].

5.3. Experimental methods

In each experiment, the crayfish (*Procambarus clarkii*, Carolina Biological) tailfan and abdominal nerve cord below the second ganglion were dissected free of the abdomen, and the connective between the fifth and sixth ganglia was desheathed. Recordings were made with a suction micropipette filled with 150 mM KCl, recording extracellularly from the axon of one or both of the photoreceptors between the fifth and sixth ganglia. The preparation was kept in van Harrevelde’s standard crayfish saline solution [van Harrevelde, 1936], at room temperature. Voltage spikes were amplified and recorded using a CED 1401 interface (Cambridge Electronic Design). Spike 2 software (CED) was used to determine spike times from the recordings. The data acquisition rate was 16667 Hz (i.e. 0.06 msec timesteps). Note that at this sampling rate our maximum error in calculating the phase of a spike within a 2π stimulus cycle may be calculated as follows. At the maximum stimulus frequency, 30 Hz, there are 33 msec per cycle, giving a possible error of 0.06 msec per 33 msec, which is equivalent to 0.18% of a 2π cycle. Thus, even at this high frequency, the phase is measured with high accuracy at this sampling rate.

Light was applied to both photoreceptors simultaneously via a halogen bulb (DDL, 20V, 160W) passed through a light pipe, with the exit of the pipe approximately 7.5 cm from sixth ganglion. For variable light levels, neutral density filters (Oriel, Stamford CT) were placed between the bulb and the light pipe. Light levels were determined using a photometer (Graseby Optronics 371 Optical Power Meter) placed as closely as possible to the location of the photoreceptor in the preparation. The spectral sensitivity of the CPR has been shown to have a maximum at 500 nm [Bruno & Kennedy, 1962]; the tungsten-halogen bulb used in the present experiments has significant spectral output in this wavelength range.

The CPR cells were positively identified as follows. Once a clear recording was obtained from a single axon in the 5–6 connective, the preparation was allowed to recover in the dark (5 nW/mm^2) for 5 min. A bright light ($22 \text{ }\mu\text{W/mm}^2$) was then turned on briefly. If the firing rate of the axon increased significantly (e.g. from 5 Hz in the dark to 30 Hz in the light) and then slowed again once the light stimulus was removed, it was determined that a CPR axon had been located.

Mechanical stimuli were applied as described in [Wilkins & Douglass, 1994; Douglass & Wilkins, 1998], by rigidly fixing the tailfan in a vertical configuration, by means of one pin through each of the

two outer uropods, to a moveable post within a room-temperature saline bath. The post, attached to an electromechanical vibration transducer (Pasco Scientific, Model SF-9324), could be moved up and down at various frequencies and amplitudes, generating relative motion between tailfan and saline solution. Due to slack in the nerve cord, there was negligible motion at the recording site. A laser Doppler vibrometer (Polytec) was used to calibrate the actual motions of the post to which the tailfan was fixed. Due to the rigid pinning between the tailfan and the post we make the reasonable assumption that there is no phase delay between the motion of the post and the motion of the tailfan.

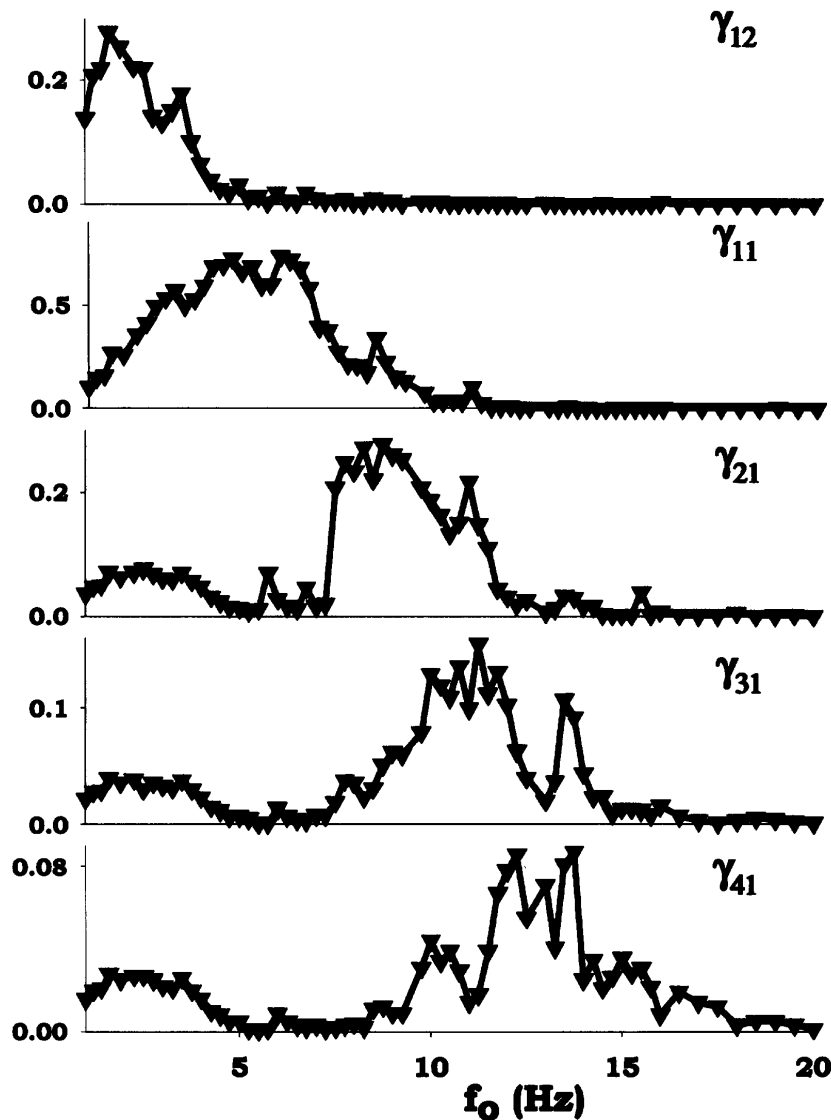


Fig. 5. Synchronization indices γ_{12} , γ_{11} , γ_{21} , γ_{31} and γ_{41} over a range of frequencies. Recordings were made at each frequency for 2 min with an amplitude of $6 \text{ }\mu\text{m}$.

The preparation was placed within a Faraday cage mounted on a vibration-isolation table (Technical Manufacturing Corporation, *MICRO-g*). Experiments were performed at room temperature ($\sim 18\text{--}22\text{ }^\circ\text{C}$). In all experiments described below, unless otherwise indicated, “dark conditions” refers to a measured light level of 5 nW/mm^2 , and “light conditions” refers to a measured value of $22\text{ }\mu\text{W/mm}^2$.

5.4. Stochastic phase synchronization in the crayfish: Higher order synchronization and Arnol’d tongues

As discussed above, in order to demonstrate synchronization in the sense of Rosenblum *et al.* [1996, 2001], it is necessary to show an increase in synchronization indices over a range of frequencies. The mechanoreceptor neurons that synapse onto the CPRs are maximally sensitive to hydrodynamic stimuli in the frequency range 5–12 Hz; we drove the tailfan preparation at frequencies of 1 to 30 Hz. At each frequency, 2 min of spikes were recorded from the photoreceptor (under dark conditions, 5 nW/mm^2). Synchronization indices for various locking ratios were then calculated at each frequency, and plotted as shown in Fig. 5. Maxima occur in γ_{12} , γ_{11} , γ_{21} , γ_{31} and γ_{41} . Note that these maxima occur at successively higher frequencies, indicating passage through a series of Arnol’d tongues [Moon, 1992]. Due to the noisiness of the system, Arnol’d tongues at 5 : 2 and other higher locking ratios were not observed.

In measurements performed in the dark on 8 crayfish driven over a range of frequencies (typically 1 to 30 Hz) with a hydrodynamic stimulus amplitude of $6\text{ }\mu\text{m}$ peak-to-peak, clear maxima in the synchronization indices were observed in all animals. While only one animal exhibited the 3 : 1 and 4 : 1 lockings shown in Fig. 5, a progression from 1 : 2 to 1 : 1 to 2 : 1 locking was observed in most cases. Exceptions included one animal where only a progression from 1 : 1 to 2 : 1 was observed, and another where only a progression from 1 : 2 to 1 : 1 was found. These results indicate that the region of 1 : 2 (2 : 1) locking was “off scale” due to the variation in frequency response from animal to animal, and thus the frequency range over which this locking occurred in these crayfish was not sampled. These results demonstrate clearly that *stochastic phase*

synchronization occurs between the CPR firing and the periodic hydrodynamic stimulus. The result also confirms that *an intrinsic oscillator does indeed exist in each CPR neuron*, since stochastic phase synchronization can only be observed between an independent oscillator and a periodic driving force.

5.5. Synchronization in dark and light

What is the effect of light on the stochastic phase synchronization between the CPR and a hydrodynamic stimulus? In four of the eight animals, the experiment illustrated in Fig. 5 was performed under both dark (5 nW/mm^2) and light ($22\text{ }\mu\text{W/mm}^2$) conditions. Recordings were made for 2 min at each stimulus frequency, as in Fig. 5. Each stimulus under light conditions was performed identically to that in the dark, except that the stimulus was not applied until the light had been on for 30 sec, in order to eliminate transients; after each light application the CPR was allowed to recover for 5 min in the dark.

Figure 6 shows γ_{12} , γ_{11} and γ_{21} respectively, with data for dark conditions shown by filled circles, and in light shown by yellow squares. As before, the frequency progression of maximal synchronization indices under dark conditions moves from γ_{12} [Fig. 6(a)] to γ_{11} [Fig. 6(b)] to γ_{21} [Fig. 6(c)].

The γ_{21} peak is at the far right of panel 6(c), at the edge of the measured frequency range, and indeed approaching a frequency range that may be out of the normal range of sensitivity of crustaceans altogether [Goodall *et al.*, 1990; Popper *et al.*, 2001]. A similar progression of maxima is observed in the light (yellow squares) for γ_{12} , γ_{11} and γ_{21} , but, for each synchronization index, the maximum occurs at a higher frequency in the light compared to the dark. This suggests that *the frequency response characteristics of the photoreceptor are shifted to higher frequencies in the light*, raising several questions whose answers may bear on fundamental problems of signal encoding. Is the higher frequency range evolutionarily related to differences in the natural frequency range of environmental stimuli to which the crayfish is subject in the light, in contrast to lower frequency stimuli it may be exposed to in the dark? Or is sensitivity to a higher frequency a dynamical result of optimal signal encoding against a background of faster CPR firing in the light? This latter possibility can

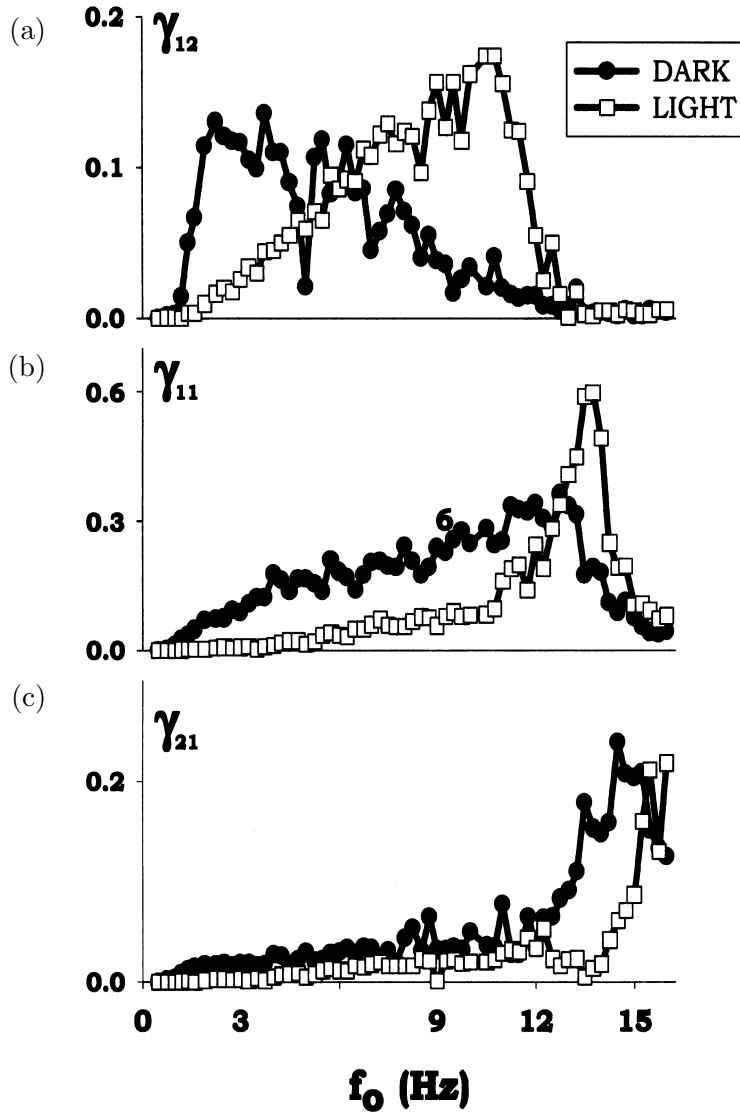


Fig. 6. Synchronization indices γ_{12} , γ_{11} and γ_{21} respectively in dark (black circles) and light (open squares). Recordings were made for 2 min at each frequency, with an amplitude of $6 \mu\text{m}$. Under light conditions ($22 \mu\text{W}/\text{mm}^2$), 5 min of rest were allowed in the dark ($5 \text{nW}/\text{mm}^2$) after each 2-min recording.

be tested using neural models where the firing rate can be realistically tuned over a 1–30 Hz range.

5.6. Stochastic synchronization and stochastic resonance

In addition to sharing a common pathway (the photoreceptor axon), these two sensory mechanisms, mechanosensitivity and light sensitivity, interact with one another. Indeed, it has been known for some time that light affects mechanosensory sensitivity. Indeed, Welsh [1934], and later Edwards [1984], demonstrated that illumination of the CPRs can elicit behavioral responses such as backwards

walking. Simon and Edwards [1990] showed that direct electrical stimulation of the CPRs leads to the same behavior.

Recently, however, Pei *et al.* [1996] made a startling observation about the photoreceptor system, demonstrating that *light enhances the encoding of weak periodic hydrodynamic stimuli*, as shown in Fig. 2(b). The signal-to-noise ratio (SNR) of a low-amplitude periodic hydrodynamic stimulus (e.g. frequency 10.5 Hz, amplitude 147 nm peak-to-peak) calculated from a power spectrum generated from a time series of delta pulses fit to the photoreceptor spike times, is enhanced as light levels are increased, up to a saturation level of $\sim 10 \mu\text{W}/\text{mm}^2$.

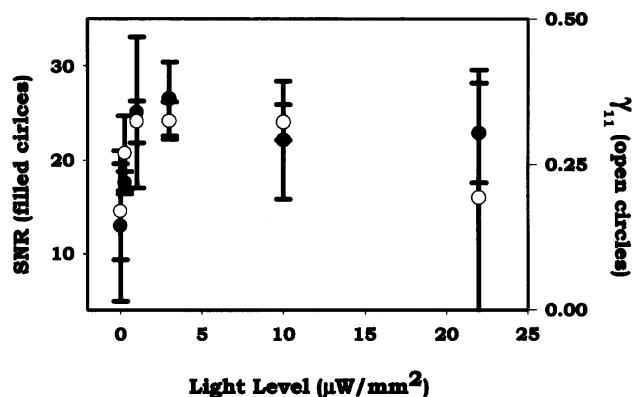


Fig. 7. SNR for a 10 Hz, 400 nm stimulus (filled circles), versus light level; γ_{11} , calculated from the same data, is shown in the open circles. Error bars show standard deviation of $N = 2$ at all light levels except the lowest, where $N = 3$.

As we have already discussed, this has been interpreted as a stochastic resonance effect, in which added light increases the noise intensity in the input signal to the photoreceptor, leading to an enhancement of the SNR [Pei *et al.*, 1996].

We have compared the increase in SNR found by Pei *et al.* [1996] with the synchronization index γ_{11} [Bahar *et al.*, 2002]. Figure 7 shows the SNR (filled circles) and γ_{11} (open circles) plotted as a function of light level, given in $\mu\text{W}/\text{mm}^2$. At each light level, the system was mechanically driven at 10 Hz and amplitude $2 \mu\text{m}$ for 2 min, then allowed to rest in the dark for at least 5 min before the application of a different light level. Figure 7 shows that the synchronization index shows a maximum at an intermediate value of light intensity (hypothesized to be related to the internal noise of the system); SNR passes through a maximum at the same light level. A maximal value of SNR as a function of input noise is a signature of stochastic resonance effects [Wiesenfeld & Moss, 1995]. Recent theoretical studies suggest that an increase in synchronization measures paralleling an increase in the SNR should be observed in stochastic resonance as well [Neiman *et al.*, 1998; Neiman *et al.*, 1999c]. To the knowledge of the authors, this is the first demonstration of the correspondence between an SR-like effect and stochastic synchronization in a biological experiment (see, however, [Mori & Kai, 2002]). While the observations shown in Fig. 7 are *consistent* with a stochastic resonance interpretation of the result described in [Pei *et al.*,

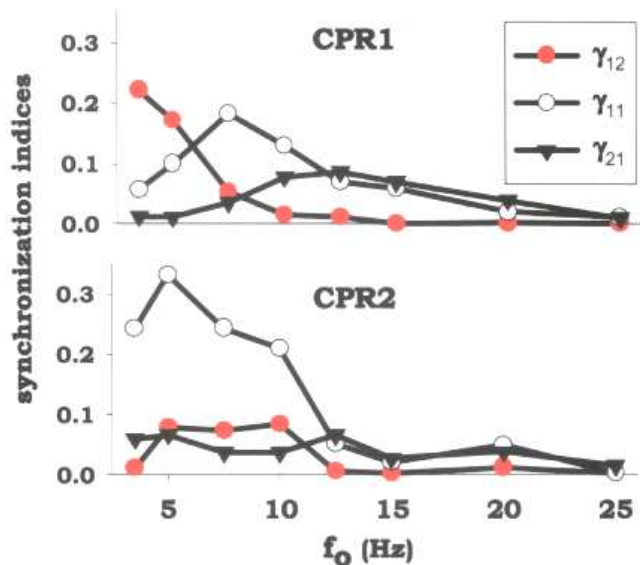


Fig. 8. Synchronization indices γ_{12} , γ_{11} and γ_{21} as functions of driving frequency f_0 for two photoreceptors (top and bottom panels, respectively) recorded simultaneously, using a driving amplitude of $6 \mu\text{m}$ under dark conditions. The spectrum of synchronization indices shows quite different behavior in one photoreceptor versus the other. Figure adapted from [Bahar, 2003].

1996], far more must be understood about the biochemical effects of light on the photoreceptors (see e.g. [Kruszewska & Larimer, 1993]) before it can be determined whether or not light increases input “noise” to these neurons.

5.7. Mutual synchronization of the two CPRs

The two photoreceptors receive excitatory input from hairs on opposite sides of the crayfish tailfan. There is no evidence of excitatory connections between the two photoreceptors [Flood & Wilkens, 1978]. Nonetheless, ablation of nerve roots providing input to one photoreceptor has been shown to decrease the response of the other CPR, indicating some possibly indirect (i.e. mediated by non-CPR interneurons) inhibitory effects between the two cells [Flood & Wilkens, 1978]. Given this observation, and that the two photoreceptors are coupled in the sense that they are subject to a common periodic mechanical stimulus, it can be asked whether the two photoreceptors (1) respond similarly to a common stimulus and (2) therefore synchronize with each other.

In order to address the first of these questions, we show in Fig. 8 the synchronization indices γ_{12} ,

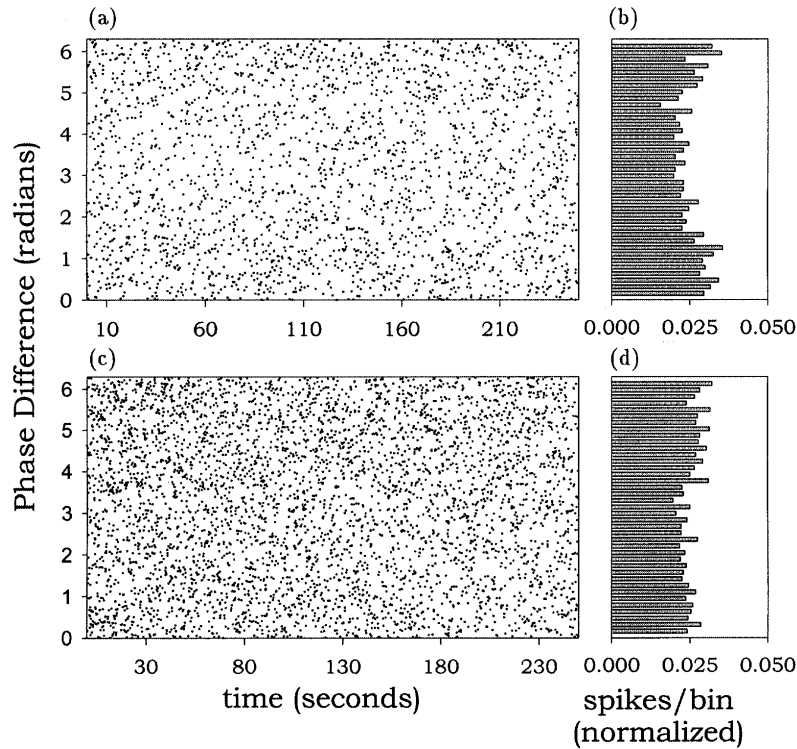


Fig. 9. Phase difference between two photoreceptors as a function of time (a), (c) and phase difference histograms (b), (d) under dark (5 nW/mm^2) and light ($22 \text{ } \mu\text{W/mm}^2$) conditions (top and bottom, respectively). Phase difference histograms are normalized to the total number of spikes in the sample. The preparation was driven with a hydrodynamic stimulus of frequency 10 Hz and amplitude $3 \text{ } \mu\text{m}$. Figure adapted from [Bahar, 2003].

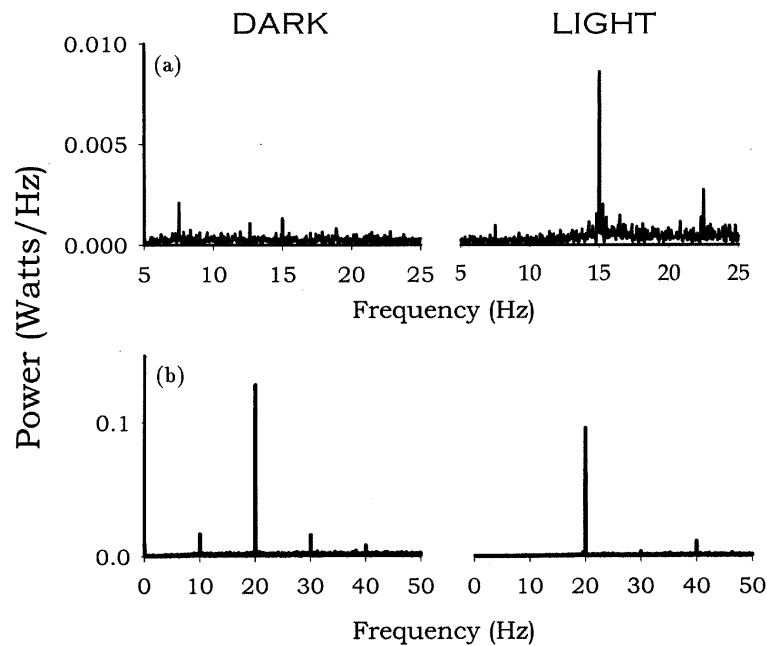


Fig. 10. (a) CPR power spectra in dark (left panel, 5 nW/mm^2) and light (right panel, $22 \text{ } \mu\text{W/mm}^2$). Stimulus frequency is 7.5 Hz, amplitude $6 \text{ } \mu\text{m}$. (b) CPR power spectra in dark (left panel, 5 nW/mm^2) and light (right panel, $22 \text{ } \mu\text{W/mm}^2$). Stimulus frequency is 10 Hz, amplitude $9 \text{ } \mu\text{m}$. Note the light-induced suppression of the odd harmonics.

γ_{11} and γ_{21} for both photoreceptors recorded simultaneously in a single crayfish, stimulated with a $6 \mu\text{m}$ sine wave under our standard dark conditions. The synchronization indices show quite different behavior in one photoreceptor versus the other. For one CPR (top panel), γ_{11} has a maximum at 7.5 Hz, while it is maximized at 5 Hz in the other CPR (lower panel).

The CPR shown in the top panel also exhibits pronounced 1 : 2 locking at low frequencies (red circles), whereas the other CPR does not. These results indicate that the two photoreceptors have different frequency responses to the same signal. This may be at least partly explained by the fact that the two photoreceptors are often observed to differ by several Hz in their intrinsic spontaneous firing rates, and entrainment by an applied stimulus likely depends in part on the frequency of the driven oscillator. The differential response may also reflect a decrease in sensitivity due to loss or damage to the motion-sensitive hairs on one side of the tailfan.

When no hydrodynamic stimulus is applied, the spontaneous firing of the two photoreceptors remains unsynchronized, see [Bahar, 2003]. Application of a common hydrodynamic stimulus, however, does introduce some synchronization between the two photoreceptor spike trains. The top panels in Fig. 9 show phase differences between the two photoreceptors, driven by a common hydrodynamic stimulus, as a function of time [panel 9(a)], and as histograms [panel 9(b)], under dark conditions (5 nW/mm^2). The bottom two panels 9(c) and 9(d) show similar measurements under light conditions ($22 \mu\text{W/mm}^2$).

Here the phase difference is calculated as in Eq. (1) with τ_i and t_k defined as the firing times of the two photoreceptors. While there are no well-defined peaks in the phase difference histograms [9(b) and 9(d)], Kolmogorov–Smirnov tests [Sokal *et al.*, 1981] show that in both cases there is a significant difference between each distribution and a control distribution generated by randomly shuffling each set of interspike intervals. In each case, $P_{\text{Ho}} < 0.0005$. Thus there does appear to be some weak synchronization between the two photoreceptors. Application of light does *not* appear to significantly change the synchronization between the two photoreceptors, however. A K–S test between the phase difference histogram in the dark [9(b)] and in the light [9(d)] gives $P_{\text{Ho}} = 0.205$, indicating that there is a significant probability that the two

distributions came from the same data set [Sokal *et al.*, 1981]. Preliminary studies also suggest that a common hydrodynamic noise field does not affect synchronization between the two photoreceptors, in contrast to neural systems such as the paddlefish electroreceptors, which exhibit synchronized bursting in response to a noisy (electrical) stimulus [Neiman & Russell, 2002]. For more discussion of the results presented in this section, see [Bahar, 2003].

6. Light Induced Rectification and Summation

In this section we show that the sixth ganglion and the CPRs are capable of rectifying and summing discharges received from the root afferents. Moreover, this operation is mediated by the light intensity. Using a simple model we quantify the action of light on the process.

6.1. *Suppression of the fundamental and amplification of the second harmonic*

In contrast to the result first reported by Pei *et al.* [1996], a novel effect is observed for higher-amplitude periodic stimuli ($\geq 2 \mu\text{m}$) [Bahar *et al.*, 2002]. Under dark (5 nW/mm^2) conditions, we observe a peak at the fundamental stimulus frequency, as shown in Fig. 10 (left panels). In the light ($22 \mu\text{W/mm}^2$), the fundamental peak (SNR_1) decreases in height, and the second harmonic (SNR_2) increases (right panels). In some animals, *all* odd harmonics are suppressed by light, as illustrated in the lower right panel.

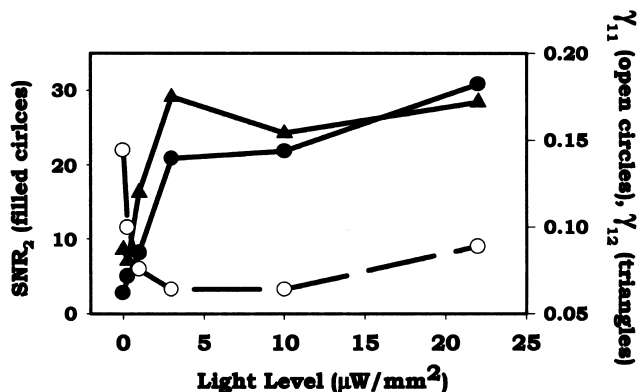


Fig. 11. SNR_2 (filled circles) versus light level (stimulus 10 Hz, $7 \mu\text{m}$). Note decrease in γ_{11} (open circles) as γ_{12} (triangles) increases.

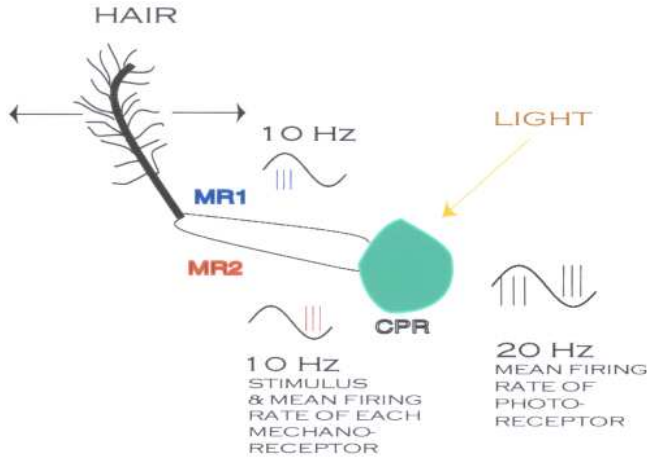


Fig. 12. Possible mechanism of full-wave rectification by the CPR. Each mechanosensory hair is innervated by two mechanoreceptor (MR) neurons, whose directional sensitivities differ by 180° [Wiese, 1976; Wiese *et al.*, 1976]. Summation of the MR inputs at the CPR is enhanced by light, accomplishing full-wave rectification of the input signal and doubling the effective stimulus frequency. Adapted from [Bahar & Moss, 2003].

We define $(\text{SNR}_2/\text{SNR}_1)_{\text{light}} > (\text{SNR}_2/\text{SNR}_1)_{\text{dark}}$ as indicative of this “second harmonic effect”. In 25 photoreceptors from 23 crayfish, stimulated with amplitudes ranging from $2 \mu\text{m}$ to $9 \mu\text{m}$ and frequencies between 7.5 Hz and 10 Hz, 13 CPRs exhibited $(\text{SNR}_2/\text{SNR}_1)_{\text{light}} > (\text{SNR}_2/\text{SNR}_1)_{\text{dark}}$. Figure 11 shows SNR_2 increasing as a function of light intensity (filled circles). We find that, in the case of this “second harmonic effect”, the γ_{11} synchronization index (open circles) *decreases* as the light level is increased, while the γ_{12} index (closed triangles) *increases*. This indicates that $1 : 2$ synchronization, which corresponds to two responses per stimulus cycle, *i.e.* a doubling of the original input frequency, increases as the second harmonic peak becomes dominant.

6.2. Light-mediated summation and the second harmonic: A model

The “second harmonic effect” can be accounted for with a simple model based on previous observations of the dual innervation of each mechanosensory hair on the tailfan by two neurons [Wiese, 1976; Wiese *et al.*, 1976]. Each neuron responds (by an increased firing rate) to the opposite half of the sinusoidal hydrodynamic displacement cycle [Wiese, 1976; Wiese *et al.*, 1976]. Figures 12 and 13 show a plausible diagrammatic scheme through which *directional rectification of the mechanical stimulus*

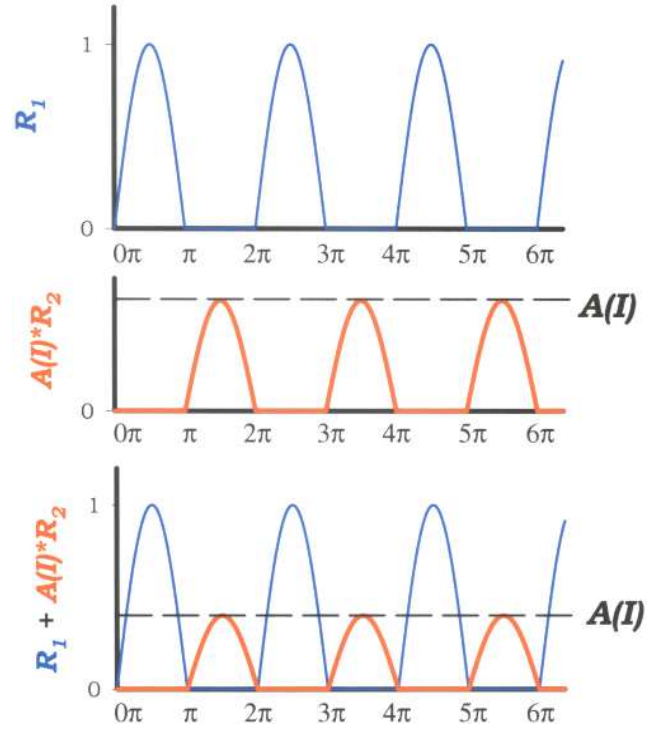


Fig. 13. Short time mean firing rate of sensory afferents R_1 (top panel) and R_2 (middle panel). The afferents respond π out of phase. The response of R_1 is normalized to unit amplitude; the response of R_2 is scaled by a factor $A(I)$, proportional to the light intensity. The bottom panel shows the result of the hypothetical summation $R_1 + A(I)R_2$, in the CPR.

by the two afferents, MR1 and MR2, and subsequent light-intensity-mediated summation in the CPR could account for our observations.

The short-time mean firing rates of the two sensory afferents, R_1 and R_2 , respond (out of phase with each other as shown in Fig. 12 and the top and middle panels of Fig. 13. Our hypothesis is that, within the CPR, these two responses are summed, and the strength of the summation, $A(I)$, is dependent on the light intensity, I . Here we have normalized the response R_1 of MR1 to unit amplitude. The response R_2 of MR2, after summation, has relative amplitude $A(I)$ with $0 \leq A \leq 1$. The result of the hypothetical summation in the CPR is shown by the response, $R_1 + A(I)R_2$, in the bottom panel of Fig. 13.

While the two responses are given by the functions:

$$\begin{aligned}
 R_1(x) &= \frac{1}{2} [\sin(x) + |\sin(x)|] \\
 A(I)R_2(x) &= \frac{A(I)}{2} [|\sin(x)| - \sin(x)],
 \end{aligned}
 \tag{6}$$

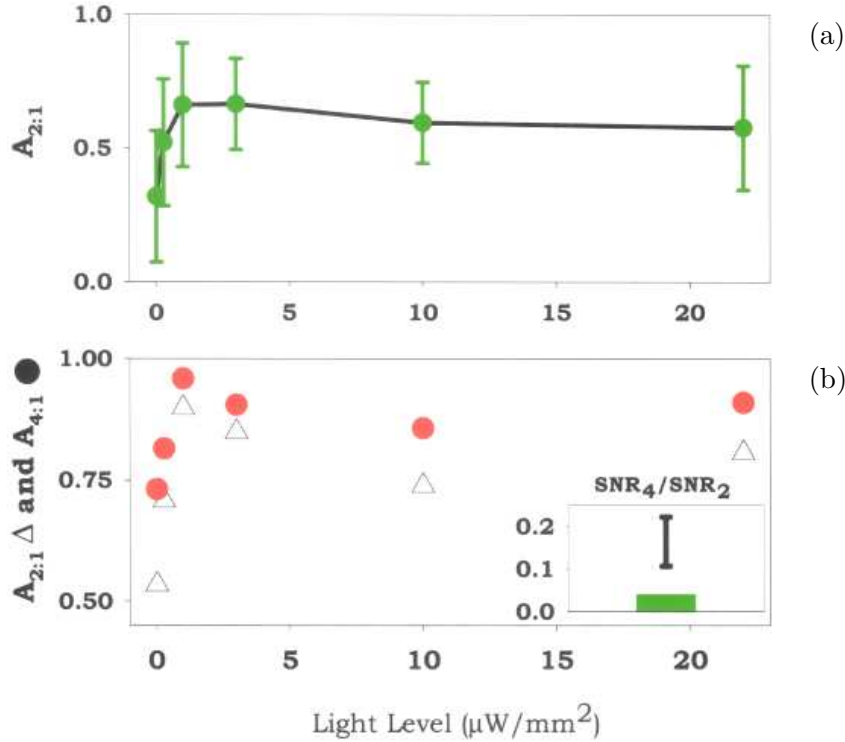


Fig. 14. (a) Calculations of $A_{2:1}(I)$ from experimental data, using Eq. (8) (filled circles). $N = 3$; error bars show standard deviation. Measurements were made in three experiments on two different crayfish, with stimulus amplitudes of $7 \mu\text{m}$, $6 \mu\text{m}$ and $2 \mu\text{m}$. Hydrodynamic stimuli were delivered at a frequency of 10 Hz. (b) Comparison of $A_{2:1}$ and $A_{4:1}$ calculated from data taken at various light levels (stimulation frequency 10 Hz, amplitude $6 \mu\text{m}$). Open triangles show $A_{2:1}$, closed circles show $A_{4:1}$. Curve is drawn through $A_{2:1}$. **Inset** shows the standard deviation of the measured ratio $\text{SNR}_4/\text{SNR}_2$, averaged over all six light levels. Our model predicts $\text{SNR}_4/\text{SNR}_2 = 1/25$, indicated by the solid bar.

it is more useful to expand these functions as Fourier series, corresponding, respectively, to the three waveforms shown in Fig. 13:

$$R_1(x) = \frac{1}{\pi} + \frac{1}{2} \sin x - \frac{2}{\pi} \left[\frac{\cos(2x)}{3} + \frac{\cos(4x)}{15} + \dots \right] \quad (7)$$

$$AR_2(x) = \frac{A}{\pi} - \frac{A}{2} \sin(x) - \frac{2A}{\pi} \left[\frac{\cos(2x)}{3} + \frac{\cos 4x}{15} + \dots \right] \quad (8)$$

$$R_1(x) + AR_2(x) = \frac{1}{\pi} (1 + A) + \frac{1}{2} (1 - A) \sin(x) - \frac{2}{3\pi} (1 + A) \cos(2x) - \frac{2}{15\pi} (1 + A) \cos(4x) - \dots \quad (9)$$

where the frequency of the stimulus is given by $x = 2\pi ft$.

The coefficients of the trigonometric terms in Eq. (9) determine the amplitudes of the peaks at corresponding frequencies in the power spectra of the neural responses. Our data indicate that the noise background is constant (within a small deviation of less than 1%) at the frequencies of the fundamental, second and fourth harmonics. Thus the ratios of the peak amplitudes in the power spectrum is given by the SNRs. For $A = 0$, the summed response predicts a power spectrum for which the fundamental peak has the largest amplitude $(1/2)^2$ followed by decreasing amplitudes for the peaks of the higher harmonics. For $A \rightarrow 1$, the fundamental peak is suppressed; the second harmonic grows in amplitude $(4/3\pi)^2$ and is followed by only the even harmonics. In all cases, the third harmonic is absent in the model. We can extract the dependence of A on light intensity by comparing the calculations with the amplitudes of the peaks in the measured power spectra.

The SNRs from the experimental data can be interpreted with the corresponding ratios of the coefficients in Eq. (9), thus,

$$\frac{\text{SNR}_2}{\text{SNR}_1} = \left[\frac{4}{3\pi} \frac{(1 + A_{2:1})}{(1 - A_{2:1})} \right]^2 \quad (10)$$

or inverting to solve for $A_{2:1}$,

$$A_{2:1} = \frac{\sqrt{\frac{\text{SNR}_2}{\text{SNR}_1} - \frac{4}{3\pi}}}{\sqrt{\frac{\text{SNR}_2}{\text{SNR}_1} + \frac{4}{3\pi}}}. \quad (11)$$

Here $A_{2:1}$ denotes the determination of $A(I)$ from the experimental measurements of the ratio of the SNRs of the second harmonic peak to the fundamental. One can obtain similar formulae for the other ratios, for example,

$$A_{4:1} = \frac{\sqrt{\frac{\text{SNR}_4}{\text{SNR}_1} - \frac{4}{15\pi}}}{\sqrt{\frac{\text{SNR}_4}{\text{SNR}_1} + \frac{4}{15\pi}}}. \quad (12)$$

Interestingly, the model predicts a light-independent constant for $A_{4:2}$, yielding the ratio $\text{SNR}_4/\text{SNR}_2 = (1/5)^2$. As we show below [inset, Fig. 14(b)], the prediction of this light independent, constant value can be used as an approximate consistency check of our model. We expect $A(I)$ to follow a course similar to SNR_2 and γ_{12} shown in Fig. 11. Figure 14 shows our determinations of $A(I)$ from the measured power spectra using Eq. (9).

We emphasize that this model is *linear*, while the transduction processes that carry the hydrodynamic mechanical stimulus to a firing rate in the CPR are almost certainly nonlinear. For example, quadratic (or higher-order) nonlinearities, or a small offset in the π phase difference between the waveforms of Fig. 13, could account for the appearance of the small third harmonic peak at 22.5 Hz in Fig. 10(a) (left panel), though the third and higher odd harmonics are absent from Eq. (7). Moreover, real data can produce a negative value for A [see error bars at lowest light level in Fig. 14(a)], because it is experimentally possible to obtain $\sqrt{\text{SNR}_2/\text{SNR}_1} < 4/3\pi$. Nevertheless, the linear model captures the gross features evident in our experimental observations.

An estimate of these inaccuracies (and a measure of the degree to which the model is not self-consistent) can be obtained by comparing the two values $A_{2:1}$, $A_{4:1}$, and checking the hypothetically constant value of $\text{SNR}_4/\text{SNR}_2$ at each light

level. Calculations of $A_{2:1}$ and $A_{4:1}$ agree well, as shown in Fig. 14(b). However, the measured value of $\text{SNR}_4/\text{SNR}_2$ is approximately 0.2, in contrast to the value predicted by the model, $1/25$ [inset, Fig. 14(b)].

7. Discussion and Summary

We hope to have convinced the reader that the crayfish mechanoreceptor system is a rich source of nonlinear dynamical and stochastic processes for experimental study. Indeed using the tailfan and CPR preparation, we have introduced SR into experimental sensory biology and found the first statistically based UPOs. Further we have been able to demonstrate that these phenomena can be extracted with statistical confidence from inherently noisy systems. In this regard, noteworthy is our demonstration of SS in the periodically forced system and in particular, our ability to extract evidence of the Arnol'd tongues from this noisy system.

In the CPR, all of these phenomena are mediated by light, and we have quantified the dependence in several cases. In particular, the influence of light on the rectification and summation processes is striking. We have generated a simple, linear model of the phenomenon of full wave rectification based on and inspired by the original observations of Wiese *et al.* [1976] of the dual enervation of the hairs. The experimental observations of the generation of second and higher even harmonics and the suppression of even harmonics in the power spectra of the spike trains measured at the CPR are clearly explained by the model. Light enhances the generation of higher even harmonics in the CPR under periodic hydrodynamic forcing. But does this phenomenon have any functional significance?

Each CPR receives inputs from ~ 70 hairs [Wilkens, 1988; Pei *et al.*, 1996], and therefore 70 afferent pairs, the situation is certain to be significantly more complex than our simple full wave rectifier model would suggest. An additional puzzle lies in the observation that enhancement of the fundamental peak occurs in the presence of light for a weak (low amplitude) periodic input signal, as described by Pei *et al.* [1996], whereas the light-induced harmonic dominance occurs predominantly for large-amplitude sinusoidal stimuli.

Both full- and half-wave rectifications have been identified in mammalian (e.g. [Rowe & Palmer, 1995; Chubb & Nam, 2000]) and invertebrate

(e.g. [Kondoh *et al.*, 1996; Okuma & Kondoh, 1996]) nervous systems. *The crayfish system, however, appears to be the first identified neural system in which full-wave rectification of one type of sensory signal is mediated by stimulation with a different type of sensory input.*

Speculations on the “use” of this effect by the crayfish in its daily routine remain open. Light-enhanced mechanical sensitivity may have evolved as an alert mechanism of periodic water motions caused by an oncoming predator when the crayfish is exposed outside its burrow [Pei *et al.*, 1996]. Rectifying this signal might relate to the sensitivity range of neurons in the higher nervous system upstream of the CPRs; a higher-frequency signal might be easier for some upstream neurons to extract from a 20–30 Hz spike train, while a lower frequency input might be more easily extractable from a spike train with a lower average frequency. If such a hypothesis is correct, these upstream neurons may provide insight into the role of the second harmonic effect within the computational apparatus of the crayfish CNS, and may ultimately suggest mammalian systems which might also exploit rectification of one sensory input, induced by another, for “computation.”

Acknowledgments

This work was supported by the U.S. Office of Naval Research, Physics Division and by the National Research Service Award from the NIH (NINDS). We are grateful to Lon A. Wilkens, David Russell, Alexander Neiman and Anke Ordemann for numerous invaluable discussions.

References

- Anishchenko, V., Moss, F., Neiman, A. & Schimansky-Geier L. [1999] “Stochastic resonance: Noise induced order,” *Uspekhi Fizicheskikh Nauk* **169**, 7–38; *Sov. Phys. Usp.* **42**, 7–36.
- Aristotle [322 BC] *The History of Animals*; see Taylor, T. [1809] *The History of Animals of Aristotle and His Treatise on Physiognomy* (Robert Wilks, London), p. 113.
- Artuso, R., Aurell, E. & Cvitanovic, P. [1990a] “Recycling of strange sets I: Cycle expansions,” *Nonlinearity* **3**, 325–338.
- Artuso, R., Aurell, E. & Cvitanovic, P. [1990b] “Recycling of strange sets II: Applications,” *Nonlinearity* **3**, 361–375.
- Bahar, S., Neiman, A., Wilkens, L. A. & Moss, F. [2002] “Phase synchronization and stochastic resonance effects in the crayfish caudal photoreceptor,” *Phys. Rev. E Rapid Commun.* **65**, 050901(R).
- Bahar, S. [2003] “Effect of light on stochastic phase synchronization in the crayfish caudal photoreceptor,” *Biol. Cybernet.*, in press.
- Bahar, S. & Moss, F. [2003] “Stochastic phase synchronization in the crayfish mechanoreceptor/photoreceptor system,” *Chaos* **13**, 138–144.
- Braun, H. A., Schäfer, K., Voigt, K., Peters, R., Bretschneider, F., Pei, X., Wilkens, L. & Moss, F. [1997] “Low-dimensional dynamics in sensory biology 1: Thermally sensitive electroreceptors of the catfish,” *J. Comput. Neurosci.* **4**, 335–347.
- Braun, H. A., Dewald, M., Schäfer, K., Voigt, K., Pei, X., Dolan, K. & Moss, F. [1999a] Low-dimensional dynamics in sensory biology 2: Facial cold receptors of the rat,” *J. Comput. Neurosci.* **7**, 17–32.
- Braun, H. A., Dewald, M., Voigt, K., Huber, M., Pei, X. & Moss, F. [1999b] “Finding unstable periodic orbits in electroreceptors, cold receptors and hypothalamic neurons,” *Neurocomput.* **26 & 27**, 79–86.
- Bruno, M. S. & Kennedy, D. [1962] “Spectral sensitivity of photoreceptor neurons in the sixth ganglion of the crayfish,” *Comput. Biochem. Physiol.* **6**, 41–46.
- Chubb, C. & Nam, J. N. [2000] “Variance of high contrast textures is sensed using negative half-wave rectification,” *Vis. Res.* **40**, 1677–1694.
- Crandall, K. A. & Fetzner, J. W. [2002] *The Crayfish Home Page*, http://zoology.byu.edu/crandall_lab/crayfish/crayhome.htm.
- Douglass, J. K., Wilkens, L., Pantazelou, E. & Moss, F. [1993] “Noise enhancement of information transfer in crayfish mechanoreceptors by stochastic resonance,” *Nature* **365**, 337–340.
- Douglass, J. K. & Wilkens, L. A. [1998] “Directional selectivities of near-field filiform hair mechanoreceptors on the crayfish tailfan (Crustacea: Decapoda),” *J. Comput. Physiol.* **A183**, 23–34.
- Edwards, D. H. [1984] “Crayfish extraretinal photoreception. I. Behavioral and motoneural responses to abdominal illumination,” *J. Exp. Biol.* **109**, 291–306.
- Flood, P. M. & Wilkens, L. A. [1978] “Directional sensitivity in a crayfish mechanoreceptive interneuron: Analysis by root ablation,” *J. Exp. Biol.* **77**, 89–106.
- Freund, J., Schimansky-Geier, L., Beisner, B., Neiman, A., Russell, D., Yakusheva, T. & Moss, F. [2002] “Behavioral stochastic resonance: How the noise from a *Daphnia* swarm enhances individual prey capture by juvenile paddlefish,” *J. Theor. Biol.* **214**, 71–83.
- Gammaitoni, L., Hänggi, P., Jung, P. & Marchesoni, F. [1998] “Stochastic resonance,” *Rev. Mod. Phys.* **70**, 223–288.
- Gingl, Z., Kiss, L. B. & Moss, F. [1995] “Non-dynamical stochastic resonance: Theory and experiments with white and arbitrarily coloured noise,” *Europhys. Lett.* **29**, 191–196.

- Goodall, C., Chapman, C. & Neil, D. [1990] "The acoustic response threshold of the Norway lobster, *Nephrops norvegicus*, in a free sound field," in *Frontiers in Crustacean Neurobiology*, eds. Wiese, K., Krenz, W.-D., Tautz, J., Reichert, H. & Mulloney, B. (Basel, Birkhäuser Verlag), pp. 106–113.
- Goychuk, I. & Hänggi, P. [2000] "Stochastic resonance in ion channels characterized by information theory," *Phys. Rev.* **E61**, 4272–4284.
- Greenwood, P. E., Ward, L. M., Russell, D. F., Neiman, A. & Moss, F. [2000] "Stochastic resonance enhances the electrosensory information available to paddlefish for prey capture," *Phys. Rev. Lett.* **84**, 4773–4776.
- Hasiotis, S. T. [1999] Crayfish fossils and burrows from the upper Triassic Chinle Formation, Canyonlands National Park, Utah. <http://www2.nature.nps.gov/grd/geology/paleo/pub/grd2/gsa24.htm>
- Hobbs, Jr. H. H. [1974] "Synopsis of the families and genera of crayfishes (Crustacea: Decapoda)," *Smithsonian Contributions to Zoology* **164**, 1–32.
- Hobbs, Jr. H. H. [1988] "Crayfish distribution, adaptive radiation and evolution," in *Freshwater Crayfish: Biology, Management and Exploitation*, eds. Holdich, D. M. & Lowery, R. S. (Timber Press, Portland), pp. 52–82.
- Hunter, J. D., Milton, J. G., Thomas, P. J. & Cowan, J. D. [1998] "Resonance effect for neural spike time reliability," *J. Neurophysiol.* **80**, 1427–1438.
- Huxley, T. H. [1880] *The Crayfish: An Introduction to the Study of Zoology* (D. Appleton, NY).
- Huygens, C. [1673] *Horologium Oscillatorium* (Parisii, France).
- Kennedy, D. [1958a] "Responses from the crayfish caudal photoreceptor," *Am. J. Ophthalm.* **46**, 19–26.
- Kennedy, D. [1958b] "Electrical activity of a 'primitive' photoreceptor," *Ann. N. Y. Acad. Sci.* **74**, 329–336.
- Kennedy, D. [1963] "Physiology of photoreceptor neurons in the abdominal nerve cord of the crayfish," *J. Gen. Physiol.* **46**, 551–572.
- Kondoh, Y., Arima, T., Okuma, J. & Hasegawa, Y. [1993] "Response dynamics and directional properties of nonspiking local interneurons in the cockroach cercal system," *J. Neurosci.* **13**, 2287–2305.
- Krasne, F. B. & Wine, J. J. [1975] "Extrinsic modulation of crayfish escape behaviour," *J. Exp. Biol.* **63**, 433–450.
- Kruszewska, B. & Larimer, J. L. [1993] "Specific second messengers activate the caudal photoreceptor of the crayfish," *Brain Res.* **618**, 32–40.
- Longtin, A., Bulsara, A. & Moss, F. [1991] "Time-interval sequences in bistable systems and the noise-induced transmission of information by sensory neurons," *Phys. Rev. Lett.* **67**, 656–659.
- McNamara, B., Wiesenfeld, K. & Roy, R. [1988] "Observation of stochastic resonance in a ring laser," *Phys. Rev. Lett.* **60**, 2626–2630.
- Miller, G. L. & Ash, S. R. [1988] "The oldest freshwater decapod crustacean, from the Triassic of Arizona," *Paleontology* **31**, 273–279.
- Moon, F. C. [1992] *Chaotic and Fractal Dynamics: An Introduction for Scientists and Engineers* (John Wiley, NY).
- Mori, T. & Kai, S. [2002] "Noise-induced entrainment and stochastic resonance in human brain waves," *Phys. Rev. Lett.* **88**, 218101.
- Moss, F., Douglass, J. K., Wilkens, L., Pierson, D. & Pantazelou, E. [1993] "Stochastic resonance in an electronic FitzHugh–Nagumo model," *Ann. N. Y. Acad. Sci.* **706**, 26–41.
- Moss, F., Pierson, D. & O’Gorman, D. [1994] "Stochastic resonance: Tutorial and update," *Int. J. Bifurcation and Chaos* **6**, 1383–1397.
- Moss, F. [1994a] "Stochastic resonance: From the ice ages to the monkey’s ear," in *Contemporary Problems in Statistical Physics*, ed. Weiss, G. H. (SIAM, Philadelphia), pp. 205–253.
- Moss, F. [1994b] "Chaos under control," *Nature* **370**, p. 596.
- Moss, F. [2000] "Stochastic resonance: Looking forward," in *Self-organized Biological Dynamics & Nonlinear Control*, ed. Walleczek, J. (Cambridge University Press, Cambridge, England), pp. 236–256.
- Neiman, A. [1994] "Synchronization-like phenomena in coupled stochastic bistable systems," *Phys. Rev.* **E49**, 3484–3487.
- Neiman, A., Silchenko, A., Anishchenko, V. & Schimansky-Geier, L. [1998] "Stochastic resonance: Noise-induced phase coherence," *Phys. Rev.* **E58**, 7118–7125.
- Neiman, A., Schimansky-Geier, L., Cornell-Bell, A. & Moss, F. [1999a] "Noise-enhanced phase synchronization in excitable media," *Phys. Rev. Lett.* **83**, 4896–4899.
- Neiman, A., Pei, X., Russell, D., Wojtenek, W., Wilkens, L. A., Moss, F., Braun, H. A., Huber, M. T. & Voigt, K. [1999b] "Synchronization of the noisy electrosensitive cells in the paddlefish," *Phys. Rev. Lett.* **82**, 660–663.
- Neiman, A., Schimansky-Geier, L., Moss, F., Shulgin, B. & Collins, J. J. [1999c] "Synchronization of noisy systems by stochastic signals," *Phys. Rev.* **E60**, 284–292.
- Neiman, A., Russell, D. F., Pei, X., Wojtenek, W., Twitty, J., Simonotto, E., Wettring, B. A., Wagner, E., Wilkens, L. A. & Moss, F. [2000] "Stochastic synchronization of electroreceptors in the paddlefish," *Int. J. Bifurcation and Chaos* **10**, 2499–2517.
- Neiman, A. B. & Russell, D. F. [2002] "Synchronization of noise-induced bursts in noncoupled sensory neurons," *Phys. Rev. Lett.* **88**, 138103.
- Okuma, J. & Kondoh, Y. [1996] "Neural circuitry underlying linear representation of wind information in

- a nonspiking local interneuron of the cockroach," *J. Comp. Physiol.* **A179**, 725–740.
- Olsen, P. E. [1977] "Stop 11, Triangle Brick Quarry," in *Field Guide to the Geology of the Durham Basin*, eds. Bain, G. L. & Harvey, B. W. (Carolina Geological Survey Fortieth Anniversary Meeting, October), pp. 59–60.
- Omberg, L., Dolan, K., Neiman, A. & Moss, F. [2000] "Detecting the onset of bifurcations and their precursors from noisy data," *Phys. Rev.* **E61**, 4848–4853.
- Ortmann, A. E. [1902] "The geographical distribution of freshwater decapods and its bearing upon ancient geography," *Proc. Amer. Philos. Soc.* **41**, 267–400.
- Packard, A. S. [1880] "Fossil crawfish from the tertiaries of Wyoming," *Amer. Naturalist* **14**, 222–223.
- Pei, X. & Moss, F. [1996] "Characterization of low dimensional dynamics in the crayfish caudal photoreceptor," *Nature* **379**, 618–621.
- Pei, X., Wilkens, L. A. & Moss, F. [1996] "Light enhances hydrodynamic signaling in the multimodal caudal photoreceptor interneurons of the crayfish," *J. Neurophysiol.* **76**, 3002–3011.
- Pei, X., Dolan, K., Moss, F. & Lai, Y.-C. [1998] "Counting unstable periodic orbits in noisy chaotic systems: A scaling relation connecting experiment with theory," *Chaos* **8**, 853–860.
- Phillips, N. S. & Edwards D. H. [1986] "Backward walking inhibits tailflip in crayfish," *Soc. Neurosci. Abstr.* **12**, p. 1207.
- Pierson, D. & Moss, F. [1995] "Detecting periodic unstable points in noisy chaotic and limit cycle attractors with applications to biology," *Phys. Rev. Lett.* **75**, 2124–2127.
- Pikovsky, A., Rosenblum, M. & Kurths, J. [2001] *Synchronization: A Universal Concept in Nonlinear Sciences* (Cambridge University Press).
- Plummer, M. R., Tautz, J. & Wine, J. J. [1986] "Frequency coding of waterborne vibrations by abdominal mechanosensory neurons in the crayfish, *Procambarus clarkii*," *J. Comput. Physiol. A Sens. Neural Behav. Physiol.* **158**, 751–764.
- Popper, A. N., Salmon, M. & Horch, K. W. [2001] "Acoustic detection and communication by decapod crustaceans," *J. Comput. Physiol.* **A187**, 83–89.
- Prosser, C. L. [1934] "Action potentials in the nervous system of the crayfish II. Response to illumination of the eye and ganglion," *J. Cell. Comput. Physiol.* **4**, 363–377.
- Rosenblum, M. G., Pikovsky, A. S. & Kurths, J. [1996] "Phase synchronization of chaotic oscillators," *Phys. Rev. Lett.* **76**, 1804–1807.
- Rosenblum, M. G., Pikovsky, A. S., Schäfer, C., Tass, P. & Kurths, J. [2001] "Phase synchronization: From theory to data analysis," in *Handbook of Biological Physics*, eds. Moss, F. & Gielen, S., *Neuro-informatics* Vol. 4, Series ed. Hoff, A. J. (Elsevier Science), Chap. 9, pp. 279–321.
- Rowe, M. H. & Palmer, L. A. [1995] "Spatio-temporal receptive-field structure of phasic W cells in the cat retina," *Vis. Neurosci.* **12**, 117–139.
- Russell, D., Wilkens, L. & Moss, F. [1999] "Use of behavioral stochastic resonance by paddlefish for feeding," *Nature* **402**, 219–223.
- Schäfer, C., Rosenblum, M. G. & Kurths, J. [1998a] "Heartbeat synchronized with ventilation," *Nature* **392**, 239–240.
- Schäfer, C., Rosenblum, M. G., Abel, H. & Kurths, J. [1998b] "Synchronization in the human cardiorespiratory system," *Phys. Rev.* **E60**, 857–870.
- Simon, T. W. & Edwards, D. H. [1990] "Light-evoked walking in crayfish: Behavioral and neuronal responses triggered by the caudal photoreceptor," *J. Com. Physiol. A Sens. Neur. Behav. Physiol.* **166**, 745–755.
- Smithsonian Museum of Natural History, Crayfish Page [2001] <http://www.nmnh.si.edu/gopher-menus/Crayfish.html>
- Sokal, R. R. & Rohlf, F. J. [1981] *Biometry*, 2nd edition (W. H. Freeman and Company, San Francisco).
- Stratonovich, R. L. [1967] *Topics in the Theory of Random Noise* (Gordon and Breach, NY), Vol. 2.
- Tass, P., Rosenblum, M. G., Weule, J., Kurths, J., Pikovsky, A. S., Volkman, J., Schnitzler, A. & Freund, J.-H. [1998] "Detection of $n:m$ phase-locking from noisy data: Application to magnetoencephalography," *Phys. Rev. Lett.* **81**, 3291–3294.
- van Harrevel, A. [1936] "A physiological solution for fresh-water crustacea," *Proc. Soc. Exp. Biol.* **34**, 428–432.
- Ward, L. M., Neiman, A. & Moss, F. [2002] "Stochastic resonance in psychophysics and in animal behavior," *Biol. Cybernet.* **87**, 91–101.
- Welsh, J. H. [1934] "The caudal photoreceptor and responses of the crayfish to light," *J. Cell. Comp. Physiol.* **4**, 379–388.
- Wiese, K. [1976] "Mechanoreceptors for near-field water displacements in crayfish," *J. Neurophysiol.* **39**, 816–833.
- Wiese, K., Calabrese, R. L. & Kennedy, D. [1976] "Integration of directional mechanosensory input by crayfish interneurons," *J. Neurophysiol.* **39**, 834–843.
- Wiesenfeld, K. & Moss, F. [1995] "Stochastic resonance: From ice ages to crayfish and SQUIDS," *Nature* **373**, 33–36.
- Wilkens, L. A. & Douglass J. K. [1994] "A stimulus paradigm for analysis of near-field hydrodynamic sensitivity in crustaceans," *J. Exp. Biol.* **189**, 263–272.
- Wilkens, L. A. & Larimer, J. L. [1972] "The CNS photoreceptor of the crayfish: Morphology

- and synaptic activity," *J. Comput. Physiol.* **80**, 389–407.
- Wilkins, L. A. [1988] "The crayfish caudal photoreceptor: Advances and questions after the first half century," *Comput. Biochem. Physiol.* **C91**, 61–68.
- Wine, J. J. [1977] "Neuronal organization of crayfish escape behavior: Inhibition of giant motoneuron via a disynaptic pathway from other motoneurons," *J. Neurophysiol.* **40**, 1078–1097.
- Wine, J. J. [1984] "The structural basis of an innate behavioral pattern," *J. Exp. Biol.* **112**, 283–320.